ADVANCED FUNCTIONAL MATERIALS
www.afm-journal.de

Materials Views
www.MaterialsViews.com

Synthesis of Phase-Pure Ferromagnetic Fe_3P Films from Single-Source Molecular Precursors

*Adam C. Colson, Chih-Wei Chen, Emilia Morosan, and Kenton H. Whitmire**

A new method for the preparation of phase-pure ferromagnetic Fe_3P films on quartz substrates is reported. This approach utilizes the thermal decomposition of the single-source precursors $H_2Fe_3(CO)_9PR$ (R = ^{t}Bu or Ph) at 400 °C. The films are deposited using a simple, home-built metal-organic chemical vapor deposition (MOCVD) apparatus and are characterized using a variety of analytical methods. The films exhibit excellent phase purity, as evidenced by X-ray diffraction, X-ray photoelectron spectroscopy, and field-dependent magnetization measurements, the results of which agree well with measurements obtained from bulk Fe_3P. Using scanning electron microscopy and atomic force microscopy techniques, the films are found to have thicknesses between 350 and 500 nm with a granular surface texture. As-deposited Fe_3P films are amorphous, and little or no magnetic hysteresis is observed in plots of magnetization versus applied field. Annealing the Fe_3P films at 550 °C results in improved crystallinity as well as the observation of magnetic hysteresis.

1. Introduction

Binary materials composed of transition metals and group 15 elements, commonly referred to as metal pnictides, have been the subject of fundamental and applied research for decades. This family of materials has drawn interest due to the wide variety of physical and chemical properties exhibited by the many possible phases. Among the more interesting of these properties are ferromagnetic and antiferromagnetic behaviors, magnetocaloric and magnetostrictive effects, and the ability to catalyze several industrially relevant reactions such as hydrodenitrogenation and hydrodesulfurization.[1–6]

Metal pnictide chemistry has experienced something of a renaissance in recent years as research groups have worked to prepare advanced metal pnictide materials such as nanoparticles and films.[7–12] Bulk metal pnictides have commonly been synthesized by reacting the pure constituent elements together at temperatures above 1000 °C.[13,14] However, these synthetic conditions are generally unsuitable for the formation of nanostructures or thin films, and a significant challenge for chemists has been the development of synthetic methodologies that allow for the formation of targeted metal pnictide phases under much milder conditions. The syntheses of several species of metal pnictide nanoparticles have been described and generally involve the thermal co-decomposition of an organometallic metal precursor with a reactive pnictide species ER_3 (E = P or As and R = H, alkyl, aryl, or silyl) in a high-boiling solvent in the presence of coordinating stabilizing agents.[7] Although considerable progress has been made using these methods, there are certain limitations that must be taken into consideration. First, phase control and nanoparticle stoichiometry can be difficult to achieve in solution, especially if one of the precursors is used in excess. Substantial empirical effort may be necessary to identify conditions under which phase control can be achieved.[15] Additionally, non-innocent interactions between the nanoparticles and stabilizing agents in solution can lead to deviations from expected nanoparticle stoichiometries.[16]

The preparation of metal pnictide films by chemical vapor deposition allows for the circumvention of some of the limitations inherent to solution-based materials processing, especially by eliminating interactions between the desired material and solvents or stabilizing agents. The majority of literature reports describing the preparation of metal pnictide films have focused on films containing early transition metals and pnictogens in a 1:1 ratio, and the preparation of metal phosphide films of most of the early transition metals has been reported by various methods.[10,17–26] Synthetic methods for the preparation of mid to late transition metal pnictide films are less well-developed, and fewer examples of completely characterized films have been described in the literature.[8,11,27–31] Several of the aforementioned syntheses have employed single-source molecular precursors, but it is worth noting that the final composition of the films did not necessarily reflect the overall stoichiometry of the precursor molecules. For example, while CoAs films prepared from 1,3-bis(*tert*-butyl)-2-(tetracarbonylcobalt)-1,3,2-diazarsolidine retained the Co:As stoichiometry of the precursor, metal-rich RuP films (P = 15–20%) were formed

A. C. Colson, Prof. E. Morosan, Prof. K. H. Whitmire
Department of Chemistry
Rice University
MS 60, 6100 Main Street
Houston, TX, 77005-1892, USA
E-mail: whitmir@rice.edu
C. W. Chen, Prof. E. Morosan
Department of Physics and Astronomy
Rice University
MS 61, 6100 Main Street
Houston, TX, 77005-1827, USA

DOI: 10.1002/adfm.201102386

upon decomposition of $H_2Ru(PMe_3)_4$.[8,30] In the former case, the presence of a covalent Co–As bond may have prevented the fragmentation of the precursor and subsequent formation of a metal-rich phase. In the latter case, the formation of metal-rich films can almost certainly be attributed to the loss of trimethylphosphine due to the increased lability of the R–P dative bond, and it should be noted that the authors had originally intended to exploit this lability in order to prepare metallic ruthenium films rather than Ru_xP_y films. These results suggest that both stoichiometry and bonding should be carefully evaluated when selecting a single-source precursor as a candidate to target a specific metal pnictide phase. Although the selection and preparation of suitable single-source precursors can be challenging, their use in thin-film preparation has several advantages. Many transition metal pnictides can be isolated in more than one phase, with each phase having a distinct stoichiometry and unique physical properties (vide infra). In order to achieve phase-purity during film preparation, the stoichiometry of the precursor materials must be carefully controlled, and this can be difficult when employing multiple precursors with different volatilities and decomposition temperatures. By contrast, single-source molecular precursors contain all of the elements required to form a targeted phase with pre-determined stoichiometry, and decomposition of single-source precursors is expected to occur in a more uniform manner under narrowly defined thermal conditions.

The preparation of advanced materials containing iron and phosphorus has been of interest to our research group for some time. The series of metal pnictide phases containing iron and phosphorus is somewhat extensive and includes Fe_3P, Fe_2P, FeP, FeP_2, and FeP_4.[13,32–35] In the bulk, Fe_3P and Fe_2P are known to be ferromagnetic, with Curie temperatures of 716 K and 217 K, respectively.[14,36] Intrigued by the prospect of preparing advanced metal pnictide materials with a relatively high ordering temperature, our research group recently attempted the solution-based synthesis of Fe_3P nanoparticles using the single-source molecular precursor $H_2Fe_3(CO)_9P^tBu$.[37] Based on the stoichiometry of the precursor, we expected that Fe_3P nanoparticles would form, but were surprised to find that Fe_2P nanostructures had instead emerged under commonly used reaction conditions. We now believe that interactions between the precursor and the stabilizing agents employed in the synthesis were responsible for the formation of iron-deficient particles. The preparation of well-characterized Fe_3P advanced materials remains a challenge.[38]

Here, we describe our efforts to overcome the limitations of solution-based Fe_3P materials synthesis and report the preparation of ferromagnetic Fe_3P films prepared by rudimentary metal-organic chemical vapor deposition (MOCVD). Films containing iron and phosphorus in a 3:1 ratio were readily deposited on quartz via thermal decomposition of volatilized $H_2Fe_3(CO)_9PR$ (R = ^{t}Bu or Ph) at 400 °C. The as-deposited films were amorphous, but could be annealed at higher temperatures in order to achieve sufficient crystallinity for characterization by X-ray analysis. The morphology of the films was studied by scanning electron microscopy and atomic force microscopy and X-ray photoelectron spectroscopy was used to examine the homogeneity of the films. Magnetic studies performed on the films confirm that the as-deposited and annealed films were both ferromagnetic, albeit with different properties.

2. Results and Discussion

Previous work has explored the possibility of preparing discrete Fe_3P nanoparticles via thermal decomposition of $H_2Fe_3(CO)_9PR$ (R = ^{t}Bu or Ph) in solution.[37] These molecules, first reported by Huttner and co-workers, seemed to us ideal candidates for single-source precursors because of their modest volatilities, the relative lability of the CO ligands, and the intimate Fe–Fe and Fe–P bonding.[39] However, we were surprised to observe the formation of Fe_2P nanoparticles when prepared in the presence of oleic acid, as the Fe_2P phase is inconsistent with the stoichiometry of the precursor. Subsequent studies have demonstrated that non-innocent interactions between the nanoparticles and oleic acid can result in the formation of metal-deficient nanoparticles.[16] While the decomposition of $H_2Fe_3(CO)_9PR$ (R = ^{t}Bu or Ph) in solution failed to yield the desired phase, bulk decomposition of the precursor was found to produce Fe_3P, and we have pursued the feasibility of preparing Fe_3P films using $H_2Fe_3(CO)_9PR$ (R = ^{t}Bu or Ph) as a single-source precursor, the description of which is reported here.

Using an independently controlled two-zone heating system (see Experimental Section), the solid $H_2Fe_3(CO)_9PR$ (R = ^{t}Bu or Ph) was sublimed at 125 °C under reduced pressure, and the gaseous material was carried through a second heating zone that had been preheated to 400 °C, whereupon the precursor underwent thermal decomposition and a metallic film was deposited on the sides of the borosilicate glass tube and onto the quartz substrates attached to the stainless steel heating stage. Film deposition at 400 °C was found to be very reproducible and good adhesion to the quartz substrate was observed, as the films passed the adhesive tape test many times over. Alternative deposition temperatures were also examined, but we observed that depositions carried out at temperatures below 400 °C generally resulted in poor substrate coating while depositions performed above 500 °C produced films that exhibited poor adhesion and were prone to flaking. The position of the heating stage was also found to be an important factor in determining the quality of the films, and the optimum position of the heating stage in the apparatus was determined empirically by varying the position over several trials until the substrates were evenly coated. Identical deposition behavior was observed for both $H_2Fe_3(CO)_9PR$ (R = ^{t}Bu or Ph) precursors.

X-ray diffraction experiments were performed on the films deposited at 400 °C but no diffracted intensity was observed, indicating that the as-deposited material was amorphous. In order to improve crystallinity, the films were flame sealed in an evacuated tube and annealed in a muffle furnace at 550 °C for four hours. X-ray diffraction patterns obtained from the annealed films closely match reference patterns obtained from bulk Fe_3P materials (**Figure 1**). The relative intensities of the reflections arising from the Fe_3P films are also similar to the intensities observed in bulk Fe_3P, suggesting that the crystallites in the film are randomly oriented with little or no preferred orientation. Unlike films prepared above 500 °C, the films that were prepared at 400 °C and annealed at 550 °C continued to exhibit good adhesion to the quartz substrates as determined by the adhesive tape test, although annealing for longer periods or at higher temperatures eventually resulted in poor adhesion and film flaking.

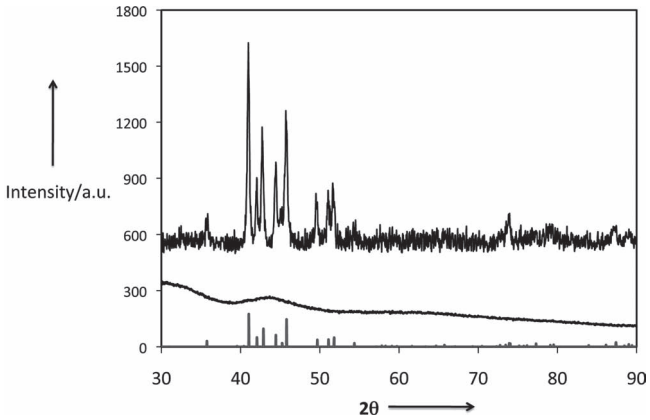

Figure 1. X-ray diffraction pattern of annealed (top) and as-deposited (bottom) Fe_3P films. The underlying line diagram shows the diffraction pattern of bulk Fe_3P (ICDD PDF# 004-2129).

Annealed and as-deposited films prepared from $H_2Fe_3(CO)_9P^tBu$ and $H_2Fe_3(CO)_9PPh$ were digested in concentrated nitric acid and the relative amounts of iron and phosphorus were determined by inductively coupled plasma optical emission spectroscopy (ICP-OES) analysis. In all cases, the iron to phosphorus ratio was found to be 3:1, indicating that both molecules were satisfactory precursors to Fe_3P materials. It should be noted that we prefer the use of $H_2Fe_3(CO)_9P^tBu$ over $H_2Fe_3(CO)_9PPh$ because the latter appears to undergo considerable decomposition when stored for extended periods of time.

The Fe_3P films were also studied by X-ray photoelectron spectroscopy (XPS) and the XPS spectra of iron and phosphorus are shown in **Figure 2**. Prior to the acquisition of the spectra, the film surfaces were sputtered with 4 keV Ar^+ ions to remove oxidized material and surface-adsorbed contaminants. The XPS spectrum of iron shows a single $2p_{3/2}$ peak at a binding energy (BE) of 706.9 eV, in precise agreement with the value reported from a high-resolution XPS analysis of bulk Fe_3P.[40] The XPS spectrum of phosphorus contains a prominent $2p_{3/2}$ peak at a BE of 129.4 eV with a $2p_{1/2}$ shoulder at a slightly higher binding energy, in good agreement with the XPS spectrum of phosphorus obtained from bulk Fe_3P.[40] A slight carbon 1s peak was observed with a BE of 284.8 and was used as a calibration reference. Integration of the carbon 1s intensity indicated that carbon comprised less than 1% of the total atomic composition of the films. The XPS spectra obtained from annealed and as-deposited Fe_3P films were indistinguishable from one another.

An XPS depth-profile was carried out on the annealed Fe_3P films in order to assess the compositional homogeneity of the deposited material. The depth profile indicates that iron and phosphorus are present in a consistent 3:1 atomic ratio throughout the entirety of the film, with the iron and phosphorus compositions dropping to zero as Ar^+ sputtering penetrates to the underlying quartz substrate (**Figure 3**), demonstrating that the film is homogeneous and free of stratification. No significant deviation in the binding energies for iron and phosphorus were observed during the depth profile.

The surface morphology and thickness of the films were analyzed by scanning electron microscopy (SEM) and atomic force

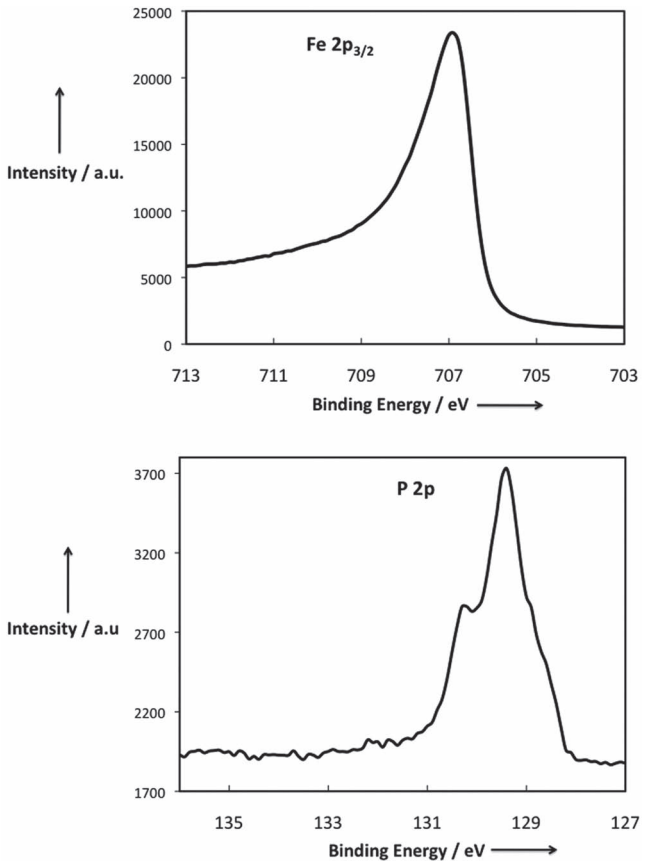

Figure 2. X-ray photoelectron spectra of Fe and P obtained from Fe_3P films.

microscopy (AFM). SEM analysis of the film surfaces revealed a granular texture, with irregularly shaped grains approximately 75–100 nm in size (**Figure 4**). Cross-sectional SEM analysis of several samples indicated that the films were between 350 and 500 nm in thickness (Figure 4). The granular texture was visible only at the surface of the films, the underlying material exhibiting a relatively featureless morphology. AFM analysis

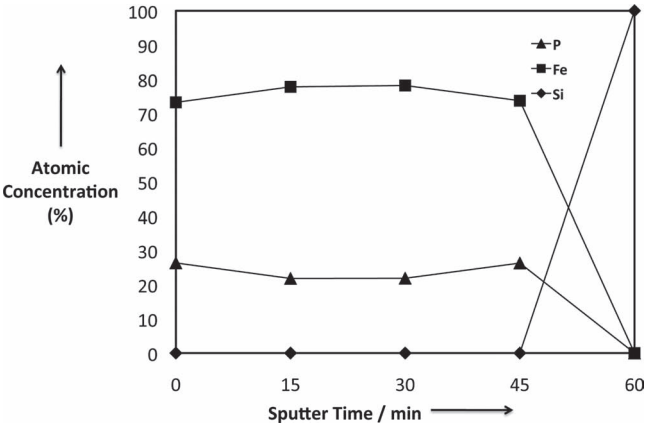

Figure 3. XPS depth profile for an annealed Fe_3P film.

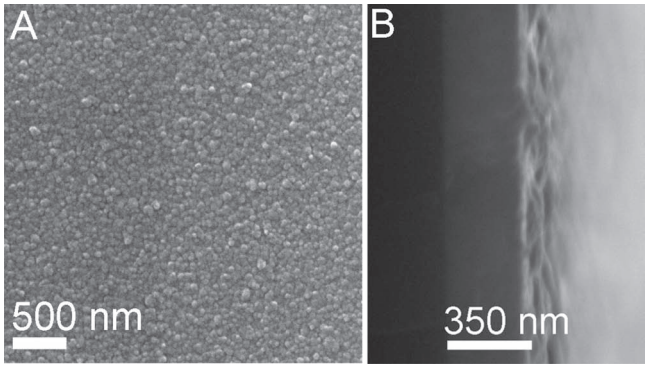

Figure 4. A) Surface and B) cross-sectional SEM images obtained from an as-deposited Fe_3P film.

demonstrates that the films had a somewhat rough texture, with some grains protruding as much as 50 nm from the surface (**Figure 5**). The annealing process had almost no effect on the morphology of the films, and the annealed and as-deposited films were virtually indistinguishable from one another based on microscopic analysis.

The attraction of both the as-deposited and annealed films to a permanent neodymium magnet provided empirical evidence of the ferromagnetic nature of the deposited material. Additionally, quantitative magnetic measurements were performed

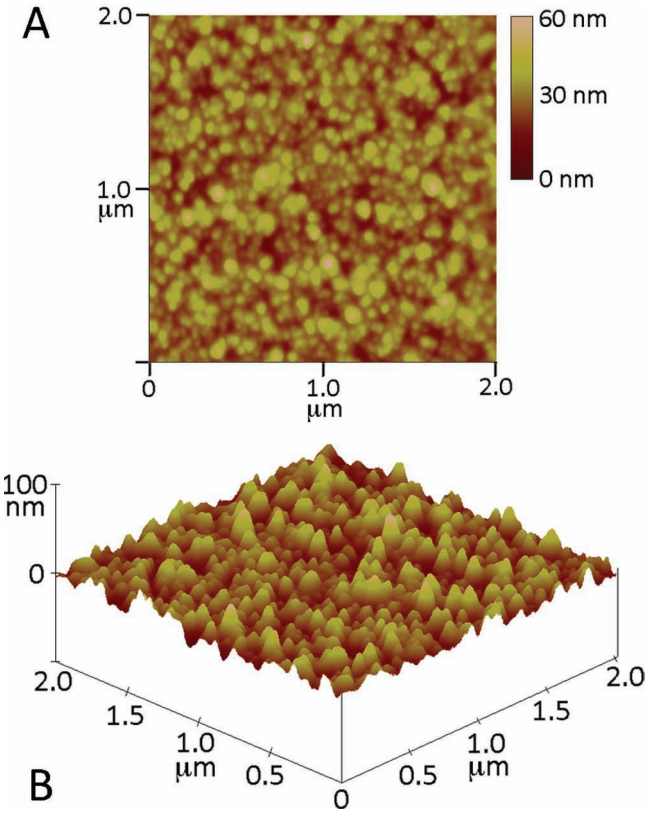

Figure 5. A) AFM images and B) height profile (tilted 20° from surface normal) obtained from an as-deposited Fe_3P film.

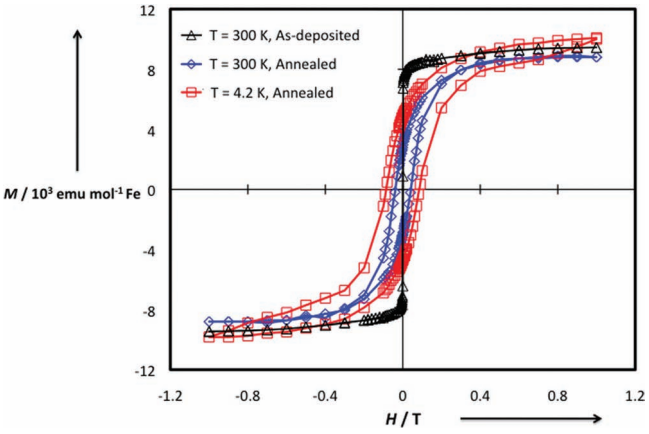

Figure 6. Magnetic hysteresis loops obtained from as-deposited and annealed Fe_3P films.

on the as-deposited and annealed films, and a plot of magnetization versus applied field is presented in **Figure 6**. The as-deposited films demonstrated ferromagnetic behavior at 300 K, although no significant hysteresis was observed. By contrast, magnetic measurements carried out on an annealed sample at temperatures of 300 K and 4.2 K resulted in well-defined, symmetrical hysteresis loops, the latter exhibiting a wider loop than the former. The magnetization shown in Figure 6 is reported in units of emu mole^{-1} iron, and the quantitative elemental analyses of the films were carried out spectroscopically using ICP-OES. The saturation magnetization of bulk Fe_3P at 4.2 K and 25 kOe was reported to be 155 emu g^{-1}.[14] This is in close agreement with the saturation magnetization of annealed Fe_3P films reported in this work, which was calculated to be 153 emu g^{-1}.

3. Conclusions

We have described the facile preparation of Fe_3P films using the conveniently synthesized single-source molecular precursors $H_2Fe_3(CO)_9PR$ (R = ^{t}Bu or Ph). Characterization by ICP-OES, XRD, and XPS indicates that the films exhibit unprecedented phase purity with no evidence of contaminant phosphide phases or metallic iron, unlike previously reported attempts at Fe_3P film synthesis.[41,42]

Brock and co-workers have recently suggested that a critical study of the magnetic properties of metal phosphide materials provides a more complete assessment of phase purity, arguing that techniques such as XRD can incorrectly imply phase purity in cases where impurities are present at low concentrations or are amorphous and undetectable by X-ray analysis.[15] In keeping with this expanded criterion for establishing phase purity, field-dependent magnetization studies were carried out on the Fe_3P films. The data obtained from annealed Fe_3P films were in close agreement with data obtained from bulk samples of Fe_3P, providing additional evidence of phase purity.

The use of single-source precursors has allowed us to prepare Fe_3P films using an extremely rudimentary MOCVD apparatus. By contrast, preparation of phase-pure Fe_3P films

using separate sources of iron and phosphorus could require considerable engineering in order to achieve co-decomposition of precursors with the correct stoichiometries and avoid the formation of phases such as Fe_2P or FeP. The films reported in this work exhibit electronic, magnetic, and crystallographic properties similar to those observed in bulk Fe_3P. This is an interesting and potentially useful observation, as bulk Fe_3P has been identified as a possible component in the preparation of semiconductor spintronic materials.[43]

As discussed previously, Fe_3P is only one of several known iron phosphide phases. The directed synthesis of phase-pure Fe_3P films using a single-source molecular precursor represents a major advance in the preparation of functional metal pnictide materials. An intriguing extension of this work would be the preparation of ternary or quaternary metal pnictides by employing single-source precursor strategies and investigations in this direction are currently underway.

4. Experimental Section

General Considerations: $H_2Fe_3(CO)_9PR$ (R = ^{t}Bu or Ph) was prepared according to previously reported procedures and was freshly crystallized and dried thoroughly under reduced pressure before use.[39] $H_2Fe_3(CO)_9PR$ (R = ^{t}Bu or Ph) can be weighed quickly in the air, but should be stored under inert gas at below –20 °C to avoid oxidation and decomposition. All films were kept under argon before and after all instrumental characterizations to prevent oxidation.

Fe_3P Film Deposition: Quartz microscope slides were obtained from Ted Pella, Inc. and were cut into approximately 1.5 cm × 2.0 cm substrates. The substrates were cleaned with acetone and ethanol and dried under inert gas. Substrates were fixed to a stainless steel heating stage using silver paste (SPI Supplies). A rudimentary horizontal hot-wall MOCVD apparatus was used for all depositions, and a schematic of the device is shown in **Figure 7**. The apparatus consists of a 25 mm × 200 mm borosilicate glass tube (Corning) coupled to a 25 mm × 100 mm borosilicate glass spacer tube via a stainless steel vacuum fitting (Ultra-Torr, Swagelok). The spacer tube was then coupled to a vacuum inlet using a second vacuum fitting. Prior to assembling the apparatus, 10 mg of $H_2Fe_3(CO)_9PR$ (R = ^{t}Bu or Ph) was loaded into the bottom of the tube, and the stainless steel heating stage was positioned as shown in the schematic. The apparatus was then connected to a high-vacuum manifold and evacuated until an attached cold-cathode ionization vacuum gauge stabilized at approximately 2×10^{-7} Torr. A 100-mm section of the apparatus (Zone 1 in Figure 7) was wrapped with fiberglass-insulated heating tape (Samox) connected to a variable transformer and embedded with a thermocouple probe. A 75 mm segment of the apparatus (Zone 2 in Figure 7) was prepared in a similar fashion, resulting in a two-zone heating system. Zone 1 was heated first, and after attaining the target temperature of 400 °C, Zone 2 was gradually heated to 125 °C. After approximately 25 min, the heating tapes were removed from Zones 1 and 2, and films with a metallic luster were found to have formed on the quartz substrates. The apparatus was immediately tilted into a vertical position and a 150 mm segment of the borosilicate tubing was flame sealed under high vacuum, isolating the heating stage and the attached substrates from the atmosphere. Selected samples were then annealed by placing the sealed tube in a muffle furnace and heating to 550 °C for 4 h.

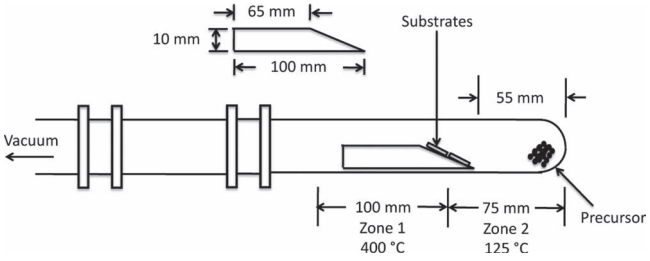

Figure 7. Schematic diagram of the home-built MOCVD apparatus employed in the deposition of Fe_3P films.

Film Characterization: Quantitative elemental analyses of iron and phosphorus were carried out using ICP-OES on a Perkin-Elmer instrument using an internal yttrium standard. The spectral emission lines at 238.204 nm and 213.617 nm were selected for analysis of iron and phosphorus, respectively. Iron was analyzed by radial plasma viewing, while phosphorus was analyzed by axial plasma viewing. The films were digested in concentrated nitric acid with sonication and diluted to a suitable concentration prior to analysis.

XPS was carried out using a Physical Electronics PHI Quantera SXM instrument using a monochromatic Al Kα source (1486.6 eV) operated at 40.7 W with a beam size of 200 μm and a take off angle of 45°. A band pass of 26 eV was used for the accurate determination of the iron $2p_{3/2}$ and phosphorus 2p binding energies and during depth profiling. The films were sputtered with an Ar^+ ion beam (4 keV) for 5 min prior to analysis to remove any surface oxidation or contaminants. A 4 keV Ar^+ ion beam was also used for sputtering during depth profile studies. The peak positions were calibrated using the 1s peak from adventitious carbon (284.8 eV).

SEM was carried out on a FEI Quanta 400 FEG microscope operated in secondary electron mode at 30 kV. SEM images were obtained on the native films, as it was not necessary to sputter-coat the films prior to imaging. The film thicknesses were determined by analyzing the cross-section of selected films. AFM images were obtained using a Digital Instrument Nanoscope IIIa microscope with a Si tip operated in tapping mode.

X-ray diffraction (XRD) data were collected on a Rigaku D/Max-2100PC powder diffractometer using unfiltered Cu Kα radiation (λ = 1.5406 Å) at 40 kV and 40 mA and a step size of 0.034°. Data processing was carried out using MDI's Jade 9.0. The powder diffraction file (PDF) for the Fe_3P phase (# 004-2129) was obtained from the International Centre for Diffraction Data (ICDD) and was used as a reference for phase identification and analysis.

The field-dependent magnetization data were collected using a Quantum Design Magnetic Property Measurement System (QD MPMS). Prior to analysis, the Fe_3P films on quartz were sectioned into pieces approximately 5.0 mm × 5.0 mm in size. Data from as-deposited samples were collected at 300 K, and data from annealed samples were collected at 300 and 4.2 K. After analysis, the samples were digested in concentrated nitric acid and the total iron and phosphorus content of each sample was quantitatively determined by ICP-OES. The diamagnetic contribution from the quartz substrate was observed to be negligible, and no further corrections to the data were applied.

Acknowledgements

The authors thank Rice University, the National Science Foundation (CHE-0719396), and the Robert A. Welch Foundation (C-0976) for funding. The authors also thank Anna T. Kelly and Sean R. Walsh for useful consultations.

Received: October 4, 2011
Revised: January 3, 2012
Published online: February 14, 2012

[1] V. A. Chernenko, L. Wee, P. G. McCormick, R. Street, *J. Appl. Phys.* **1999**, *85*, 7833.
[2] O. Tegus, E. Brück, L. Zhang, Dagula, K. H. J. Buschow, F. R. de Boer, *Physica B* **2002**, *319*, 174.

[3] A. F. Gaudette, A. W. Burns, J. R. Hayes, M. C. Smith, R. H. Bowker, T. Seda, M. E. Bussell, *J. Catal.* **2010**, *272*, 18.
[4] A. W. Burns, A. F. Gaudette, M. E. Bussell, *J. Catal.* **2008**, *260*, 262.
[5] S. T. Oyama, *J. Catal.* **2003**, *216*, 343.
[6] K. Senevirathne, A. W. Burns, M. E. Bussell, S. L. Brock, *Adv. Funct. Mater.* **2007**, *17*, 3933.
[7] S. L. Brock, K. Senevirathne, *J. Solid State Chem.* **2008**, *181*, 1552.
[8] J. Shin, A. Waheed, K. Agapiou, W. A. Winkenwerder, H.-W. Kim, R. A. Jones, G. S. Hwang, J. G. Ekerdt, *J. Am. Chem. Soc.* **2006**, *128*, 16510.
[9] A. N. Gleizes, *Chem. Vap. Deposition* **2000**, *6*, 155.
[10] C. S. Blackman, C. J. Carmalt, T. D. Manning, S. A. O'Neill, I. P. Parkin, L. Apostolico, K. C. Molloy, *Chem. Vap. Deposition* **2003**, *9*, 10.
[11] A. Panneerselvam, M. A. Malik, M. Afzaal, P. O'Brien, M. Helliwell, *J. Am. Chem. Soc.* **2008**, *130*, 2420.
[12] A. E. Henkes, R. E. Schaak, *Chem. Mater.* **2007**, *19*, 4234.
[13] D. Bellavance, M. Vlasse, B. Morris, A. Wold, *J. Solid State Chem.* **1969**, *1*, 82.
[14] R. Gambino, *J. Appl. Phys.* **1967**, *38*, 1253.
[15] E. Muthuswamy, P. R. Kharel, G. Lawes, S. L. Brock, *ACS Nano* **2009**, *3*, 2383.
[16] A. C. Colson, K. H. Whitmire, *Chem. Mater.* **2011**, *23*, 3731.
[17] S. E. R. Hiscocks, J. B. Mullin, *J. Mater. Sci.* **1969**, *4*, 962.
[18] C. S. Blackman, C. J. Carmalt, S. A. O'Neill, I. P. Parkin, L. Apostolico, K. C. Molloy, *Chem. Mater.* **2004**, *16*, 1120.
[19] C. S. Blackman, C. J. Carmalt, S. A. O'Neill, I. P. Parkin, K. C. Molloy, L. Apostolico, *J. Mater. Chem.* **2003**, *13*, 1930.
[20] S. Motojima, T. Wakamatsu, K. Sugiyama, *J. Less-Common Met.* **1981**, *82*, 379.
[21] I. M. Watson, J. A. Connor, R. Whyman, *Thin Solid Films* **1991**, *196*, L21.
[22] C. S. Blackman, C. J. Carmalt, T. D. Manning, I. P. Parkin, L. Apostolico, K. C. Molloy, *Appl. Surf. Sci.* **2004**, *233*, 24.
[23] J. T. Scheper, K. C. Jayaratne, L. M. Liable-Sands, G. P. A. Yap, A. L. Rheingold, C. H. Winter, *Inorg. Chem.* **1999**, *38*, 4354.
[24] T. Thomas, C. S. Blackman, I. P. Parkin, C. J. Carmalt, *Eur. J. Inorg. Chem.* **2010,**5629.
[25] R. G. Palgrave, I. P. Parkin, *New J. Chem.* **2006**, *30*, 505.
[26] S. T. Lewkebandara, C. H. Winter, *Chem. Vap. Deposition* **1996**, *2*, 75.
[27] J. Choi, S. Choi, M. H. Sohn, H. Park, Y. Park, H.-M. Park, S. C. Hong, S. Cho, *J. Magn. Magn. Mater.* **2006**, *304*, e112.
[28] P. J. Walsh, N. Bottka, *J. Electrochem. Soc.* **1984**, *131*, 444.
[29] A. Panneerselvam, C. Q. Nguyen, J. Waters, M. A. Malik, P. O'Brien, J. Raftery, M. Helliwell, *Dalton Trans.* **2008**, 4499.
[30] F.-R. Klingan, A. Miehr, R. A. Fischer, W. A. Herrmann, *Appl. Phys. Lett.* **1995**, *67*, 822.
[31] M. Solzi, C. Pernechele, M. Ghidini, M. Natali, M. Bolzan, *J. Magn. Magn. Mater.* **2010***322*, 1565.
[32] J. Gopalakrishnan, S. Pandey, K. K. Rangan, *Chem. Mater.* **1997**, *9*, 2113.
[33] F. Hulliger, *Struct. Bond.* **1968**, *4*, 83.
[34] G. Boda, B. Stenström, V. Sagredo, O. Beckman, B. Carlsson, S. Rundqvist, *Phys. Scr.* **1971**, *4*, 132.
[35] M. Sugitani, N. Kinomura, M. Koizumi, S. Kume, *J. Solid State Chem.* **1978**, *26*, 195.
[36] H. Fujii, Y. Uwatoko, K. Motoya, Y. Ito, T. Okamoto, *J. Phys. Soc. Jpn.* **1988**, *57*, 2143.
[37] A. T. Kelly, I. Rusakova, T. Ould-Ely, C. Hofmann, A. Lüttge, K. H. Whitmire, *Nano Lett.* **2007**, *7*, 2920.
[38] K. L. Stamm, S. L. Brock, *J. Alloys Compd.* **2008**, *453*, 476.
[39] G. Huttner, J. Schneider, G. Mohr, J. Von Seyerl, *J. Organomet. Chem.* **1980**, *191*, 161.
[40] P. E. R. Blanchard, A. P. Grosvenor, R. G. Cavell, A. Mar, *Chem. Mater.* **2008**, *20*, 7081.
[41] S. K. Zečević, J. B. Zotović, S. L. Gojković, V. Radmilović, *J. Electroanal. Chem.* **1998**, *448*, 245.
[42] K. Kamei, Y. Maehara, *J. Appl. Electrochem.* **1996**, *26*, 529.
[43] S. J. Pearton, C. R. Abernathy, D. P. Norton, A. F. Hebard, Y. D. Park, L. A. Boatner, J. D. Budai, *Mater. Sci. Eng., R* **2003**, *40*, 137.